IOPscience iopscience.iop.org

Home Search Collections Journals About Contact us My IOPscience

Electron energy-loss spectroscopy of strongly correlated systems in infinite dimensions

This article has been downloaded from IOPscience. Please scroll down to see the full text article.

2000 J. Phys.: Condens. Matter 12 7647

(http://iopscience.iop.org/0953-8984/12/34/310)

View the table of contents for this issue, or go to the journal homepage for more

Download details:
IP Address: 171.66.16.221
The article was downloaded on 16/05/2010 at 06:42

Please note that terms and conditions apply.

J. Phys.: Condens. Matter **12** (2000) 7647–7654. Printed in the UK PII: S0953-8984(00)11828-4

Electron energy-loss spectroscopy of strongly correlated systems in infinite dimensions

Luis Craco† and Mukul S Laad‡

† Instituto de Fisica 'Gleb Wataghin'—UNICAMP, CP 6165, 13083-970 Campinas—SP, Brazil
‡ Institut für Theoretische Physik, Universität zu Köln, Zülpicher Strasse, 50937 Köln, Germany

Received 14 February 2000, in final form 23 June 2000

Abstract. We study the electron energy-loss spectra of strongly correlated electronic systems doped away from half-filling using dynamical mean-field theory ($d = \infty$). The formalism can be used to study the loss spectra in the optical ($\boldsymbol{q} = 0$) limit, where it is simply related to the optical response, and hence can be computed in an approximation-free way in $d = \infty$ dimensions. We apply the general formalism to the one-band Hubbard model away from $n = 1$, with inclusion of site-diagonal randomness to simulate effects of doping. The interplay between the coherence-induced plasmon feature and the incoherence-induced high-energy continuum is explained in terms of the evolution in the local spectral density upon hole doping. Inclusion of static disorder is shown to result in qualitative changes in the low-energy features, in particular to the overdamping of the plasmon feature, resulting in a completely incoherent response. The calculated lineshapes of electron energy-loss spectra are compared to the lineshapes of experimentally observed spectra for the normal state of the high-T_c materials near optimal doping and good qualitative agreement is found.

The ac conductivity and dielectric tensor provide valuable information concerning the finite-frequency, finite-temperature charge dynamics of an electronic fluid in a metal. The dramatic changes in the electronic state from localized to itinerant across an insulator–metal (I–M) transition, be it driven by pressure or by doping the insulator, are reflected in concomitant changes in the optical responses. These studies, therefore, give one a systematic picture describing the nature of the change in the electronic state, the appearance of new low-energy excitations, and their dispersion and stability. For cuprate superconductors, for example, these studies have convincingly demonstrated the non-Fermi-liquid nature of the charge [1] and spin [2] dynamics in the normal state.

The optical response of a solid provides an estimate of the carrier scattering rate at finite frequency, and thus gives detailed information about the finite-frequency collective excitations responsible for scattering the carriers. In a quantum paramagnetic metal, the dominant carrier scatterers are electron–hole pairs, which are the low-energy collective excitations—it is precisely the e–h spectrum which is measured by electron energy-loss spectroscopy (EELS) which provides one with a direct experimental picture of the spectral density of particle–hole excitations in a solid [3].

In a weakly interacting system, one expects the details of the particle–hole spectrum to be sensitive to details of the shape and size of the Fermi surface (e.g., its curvature). That such a picture is untenable for strongly correlated systems was pointed out by Shastry *et al* [4], who argued that in this case, the whole Brillouin zone tends to get populated. Another important

0953-8984/00/347647+08$30.00 © 2000 IOP Publishing Ltd

point of considerable relevance is the transfer of spectral weight over large energy scales that is characteristic of strongly correlated systems—it has no analogue in weakly interacting Fermi systems. Consequently, one expects qualitatively different responses in this case, compared to those characteristic of weakly interacting systems.

Quite generally, the transmission EELS lineshape is related to the wave-vector- and frequency-dependent dielectric function via the equation

$$I(\boldsymbol{q},\omega) = -\mathrm{Im}\,\frac{1}{\epsilon(\boldsymbol{q},\omega)}. \tag{1}$$

Following reference [3], we employ the random-phase approximation (RPA) to treat the small-$\boldsymbol{q}$ part. In the optical limit that we are interested in ($q \to 0$),

$$\epsilon(\boldsymbol{q}\to 0,\omega) = 1 + 4\pi\,\frac{\mathrm{i}\sigma(\omega)}{\omega}$$

where $\sigma(\omega)$ is the longitudinal optical conductivity. The analysis carried out along these lines is invalid when $qa \simeq 1$, where the short-ranged part of the potential has to be considered and the RPA is inadequate. However, local correlation effects are correctly incorporated into the above equation via $\sigma(\omega)$, which can be computed reliably with $d = \infty$, for example. In this limit, $\boldsymbol{q} \simeq 0$, the particle–hole spectral density is obtainable from the dissipative part of [3]:

$$I(0,\omega) = -\mathrm{Im}\,\frac{1}{\epsilon(0,\omega)} = \frac{\epsilon''(\omega)}{\epsilon'^2(\omega)+\epsilon''^2(\omega)} \tag{2}$$

with

$$\epsilon'(\omega) = 1 - \frac{4\pi\sigma''(\omega)}{\omega} \qquad \epsilon''(\omega) = \frac{4\pi\sigma'(\omega)}{\omega}$$

so one needs to have an estimate of the longitudinal dielectric constant to calculate the EELS spectrum. It is to be noted that this yields the EELS lineshape corresponding to the experiment performed in the so-called 'transmission mode'. Thus, the problem has now been reduced to that of computing $\epsilon(\omega)$, which, being a local quantity, can be computed in an approximation-free way for $d = \infty$ [5].

In this communication, we want to develop a theory of the transmission EELS (equation (1)) for electronic systems which undergo Mott transitions as a function of band filling [5]. To be specific, we consider the one-band Hubbard model, where the Mott transition can be driven by hole doping the Mott insulator, or by pressure (which changes the ratio U/t). To capture more fully the effects of chemical substitution (which is how doping is carried out in practice), we also introduce static, site-diagonal disorder in the model. The resulting Hamiltonian is

$$H = -\sum_{ij\sigma} t_{ij} c^{\dagger}_{i\sigma} c_{j\sigma} + U\sum_{i} n_{i\uparrow}n_{i\downarrow} - \sum_{i,\sigma}(v_i - \mu)n_{i\sigma} \tag{3}$$

as a prototype model describing the electronic degrees of freedom in TM oxides. To study the 3D case, we employ the $d = \infty$ approximation, which is the best among those currently available to study the M–I transition [5]. Since this method has been extensively reviewed, we only summarize the relevant aspects. All transport properties, which follow from the conductivity tensor, are obtained from a $\boldsymbol{k}$-independent self-energy for $d = \infty$; the only information about the lattice structure comes from the free band dispersion in the full Green function:

$$G(k,\omega) = G(\epsilon_k,\omega) = \frac{1}{\omega + \mu - \epsilon_k - \Sigma(\omega)}. \tag{4}$$

Solving the model for $d = \infty$ requires a reliable way to solve the single-impurity Anderson model (SIAM) embedded in a dynamical bath described by the hybridization function, $\Delta(\omega)$. There is an additional condition that completes the self-consistency:

$$\int \mathrm{d}\epsilon\ G(\epsilon, \mathrm{i}\omega)\rho_0(\epsilon) = \frac{1}{\mathrm{i}\omega + \mu - \Delta(\mathrm{i}\omega) - \Sigma(\mathrm{i}\omega)} \tag{5}$$

where $\rho_0(\epsilon)$ is the free DOS ($U = 0$). The above equations (3), (4) refer to the disorder-free Hubbard model. With microscopic, binary disorder (which is the only type that we consider here):

$$P(v_i) = (1 - x)\delta(v_i) + x\delta(v_i - v) \tag{6}$$

only the disorder-averaged quantities are physically observable. In this case, we use an extended version of the iterated perturbation theory (IPT), which combines the effects of dynamical correlations (via usual IPT) with those of disorder (via the CPA) in a self-consistent way. For the sake of completeness, we outline the calculational details briefly. As a first step, we compute the full local Green function for the pure model using IPT. This has been shown [5] to yield results in excellent agreement with those obtained from exact-diagonalization techniques. This IPT propagator is then corrected for repeated scattering from local disorder by computing the new self-energy from the usual CPA [6]:

$$\langle T_{ii}[\Sigma(\omega)]\rangle_c = \frac{-(1 - x)\Sigma(\omega)}{1 + \Sigma(\omega)G(\omega)} + \frac{x(v - \Sigma(\omega))}{1 - (v - \Sigma(\omega))G(\omega)} = 0 \tag{7}$$

which results in an implicit equation for the interaction- and disorder-corrected self-energy (and Green function). To make the treatment self-consistent, we compute the new IPT self-energy using the new GF computed with the IPT + CPA in the first step. This procedure is repeated until convergence is achieved. At each step of the iteration, we fix the chemical potential from the Luttinger sum rule:

$$n = \int_{-\infty}^{\mu} \rho(\omega)\ \mathrm{d}\omega = x.$$

This extended IPT yields the local propagator, $\langle G_{ii}(\omega)\rangle$, corrected both for dynamical correlations and disorder-induced repeated scattering, both treated on the same footing [6]. For $d = \infty$, this is sufficient for computing the transport, because the vertex corrections in the Bethe–Salpeter equation for the conductivity vanish identically in this limit [7]. Thus, the conductivity is fully determined by the basic bubble diagram made up of fully interacting local GFs of the lattice model.

The optical conductivity and the Hall conductivity are computable in terms of the full $d = \infty$ GFs as follows [7]:

$$\sigma_{xx}(\mathrm{i}\omega) = \frac{1}{\mathrm{i}\omega} \int \mathrm{d}\epsilon\ \rho_0(\epsilon) \sum_{i\nu} G(\epsilon, \mathrm{i}\nu)G(\epsilon, \mathrm{i}\nu + \mathrm{i}\omega). \tag{8}$$

The dynamical dielectric constant is directly calculated from the optical conductivity via

$$\epsilon_{xx}(\omega) = 1 + \frac{4\pi}{\omega}\mathrm{i}\sigma_{xx}(\omega) \tag{9}$$

yielding its real and imaginary parts. Use of equation (3) then permits us to study

$$I_{EELS}(\omega) = -\mathrm{Im}\,\frac{1}{\epsilon(\omega)}.$$

Before embarking on a description of our results and their analysis, it is instructive to summarize what is known about the $d = \infty$ Hubbard model. At large U/t, and away from

half-filling ($n = 1$), the ground state is a paramagnetic FL if one ignores the possibility of symmetry breaking towards antiferromagnetism, as well as disorder effects, which are especially important near $n = 1$. This can be achieved formally by introducing a nnn hopping, which for $d = \infty$ leaves the free DOS essentially unchanged [5]. This metallic state is characterized by two energy scales: a low-energy coherence scale T_{coh}, below which local FL behaviour sets in [5], and a scale $O(D)$ (D is the free bandwidth), characterizing high-energy, incoherent processes across the remnant of the Mott–Hubbard insulator at $n = 1$. At $T < T_{coh}$, the quenching of the local moments leads to a response characteristic of a FL at small $\omega \ll 2D$ (but with the dynamical spectral weight transfer with doping, a feature of correlations), but at higher $T > T_{coh}$, the picture is that of carriers scattered off by effectively local moments, which makes the system essentially like a non-FL (note that a metal with disordered local moments is not a FL).

The picture is modified drastically in the presence of static, diagonal disorder, in which case the extended IPT has to be used. For weak disorder, the above picture is qualitatively unaffected, and the only interesting features are that Luttinger's theorem is violated, and the FL quasiparticles acquire a finite lifetime at μ [6]. However, with increasing disorder, repeated scattering effects destroy the quasiparticle picture, and the metallic state is characterized by an incoherent, non-FL response with a pseudogap structure in the DOS. Similar results were obtained earlier in reference [8], where a T-matrix approximation was employed to treat disorder-induced resonant scattering. The above describes the competing tendencies of the correlation-induced low-temperature coherence scale, T_{coh}, in the $d = \infty$ Hubbard model, and the disorder-induced incoherence, which tends to suppress it, driving it eventually to zero, leading to a non-FL metal state. A large enough disorder strength leads to band splitting, as in the usual CPA, leading to a continuous transition to a disorder-driven insulating state.

Armed with this information, we are ready to discuss our results. We choose a Gaussian unperturbed DOS, and $U/D = 3.0$ to access the strongly correlated FL metallic state away from $n = 1$, ignoring the possible instability to an AF-ordered phase. All calculations are performed at a low temperature, $T = 0.01D$. We are mainly interested in the variation of the EELS lineshape with hole doping, given here by $\delta = (1-n)$. This fixes the chemical potential, and the FL resonance position, and the IPT describes the evolution of spectral features in good agreement with exact-diagonalization studies [5]. In view of the ability of the IPT to reproduce all the qualitative aspects observed in $\sigma_{xx}(\omega)$, we believe that it is a good tool in the present case. Figure 1 shows the optical conductivity and the longitudinal dielectric constant. $\sigma_{xx}(\omega)$ agrees with calculations performed earlier in all the main respects; in particular, it clearly exhibits the low-energy quasicoherent Drude form, the transfer of optical spectral weight from the high-energy, upper-Hubbard-band states to the low energy, band-like states with increasing hole doping, and the isosbectic point at which *all* the $\sigma_{xx}(\omega)$ curves as functions of filling cross at one point, to within numerical accuracy. It is interesting to note that such features have also been observed in experimental studies†. Correspondingly, $\mathrm{Im}\,\epsilon_{xx}(\omega)$ also shows the isosbectic point, the explanation for which is identical to the heuristic one proposed recently by us for the case of $\sigma_{xx}(\omega)$ [10].

In figures 2 and 3, we show the theoretically calculated EELS spectra for $U/D = 3.0$ and for different band fillings as functions of disorder strength, v. This allows us to access the intermediate-correlation regime, where the absence of any small parameter in the problem requires the use of controlled methods that interpolate correctly between the weak- and strong-coupling limits (such as the $d = \infty$ method used here). From the calculation of the optical response, we have checked that $\mathrm{Im}\,\sigma_{xx}(\omega = 0) = 0$, implying that $-\mathrm{Re}\,1/\epsilon(0) = 0$, as

† See, for example, the various cases discussed in the review of reference [2].

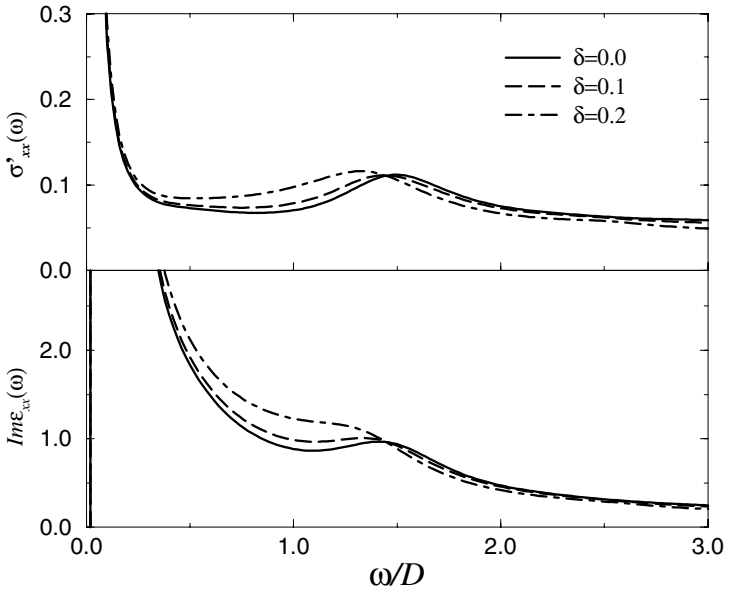

Figure 1. The real part of the optical conductivity σ_{xx} for $U/D = 3.0$, $\delta = 0.1$ (continuous) and $\delta = 0.2$ (dot–dashed). The lower panel shows the imaginary dielectric constant for the same parameter values. Note that there is an isosbectic point for each of the quantities.

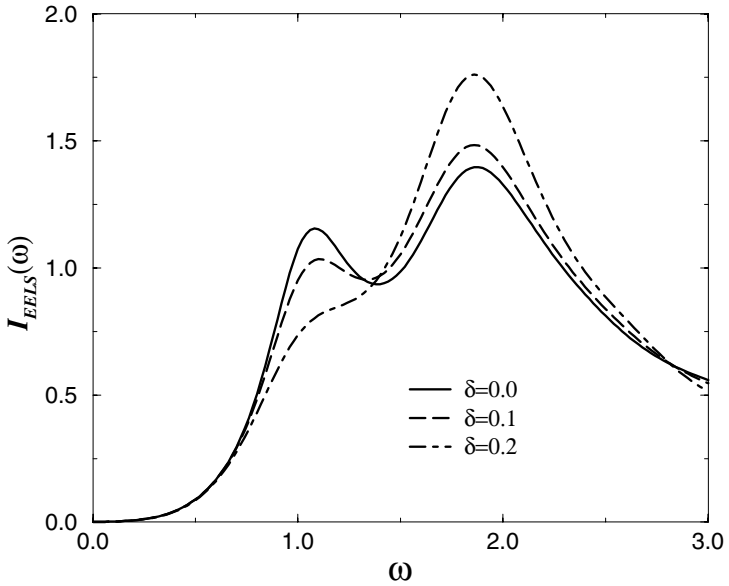

Figure 2. The electron energy-loss spectra for the doped Hubbard model for $U/D = 3.0$, and $\delta = 0.1, 0.2, 0.3$ as shown.

required [11]. With $U/D = 3.0$, we observe a peak at $\omega \simeq U/2$, associated with the transitions from the lower Hubbard band to the quasiparticle resonance. We associate this peak with the strongly renormalized particle–hole excitations in the strongly correlated metal. In this context, two features are worthy of mention: at low energy, the loss intensity goes quadratically with

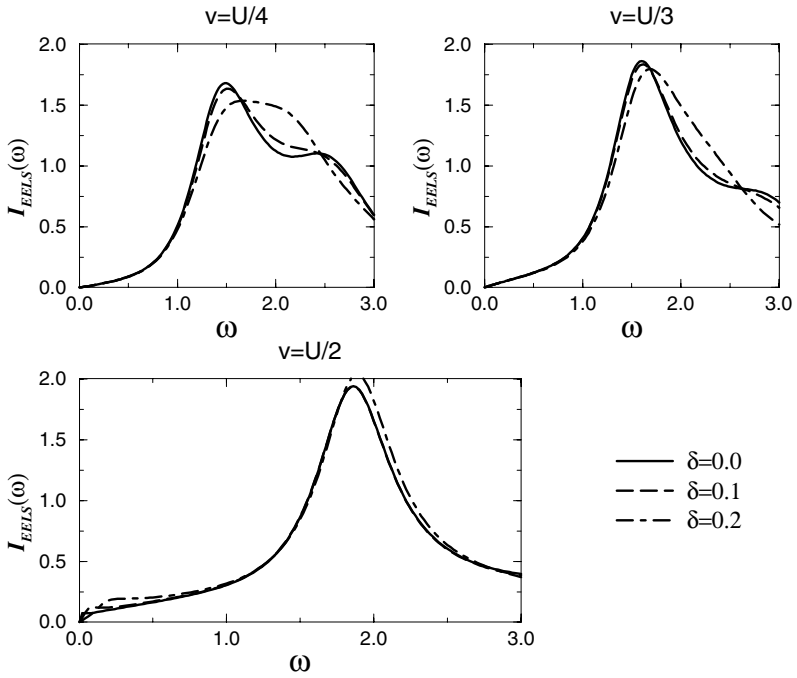

Figure 3. The EELS spectra for the $d = \infty$ Hubbard model for $U/D = 3.0$ and $v/U = 1/4, 1/3, 1/2$. See the text for the explanation of various structures in $I_{EELS}(\omega)$ in the light of the underlying structure of the local spectral density of the Hubbard model for $d = \infty$.

ω, and the particle–hole peak position shifts with increasing doping. The shift of this feature correlates with that of the mid-IR peak in the optical conductivity (figure 1), and is thus a clear manifestation of the transfer of optical weight to lower energy with hole doping. Moreover, appreciable loss intensity is observed at higher energies ($\omega > 2.0$) as a smooth continuum, in contrast to the expectations from a weakly correlated (with very small U/D) FL. This clearly shows how the delicate balance between coherence and incoherence is controlled by the transfer of optical spectral weight in the full EELS spectrum. In fact, we expect the coherent feature in the full spectrum to become sharper as T ($0.01D$ in our analysis) is lowered further. We see from the above that coupling to high-energy, incoherent, multiparticle excitations strongly renormalizes, but does not destroy, the coherent response in a strongly correlated Fermi liquid. However, the analysis presented above shows that a proper treatment of coherence (related to itineracy) and incoherence (coming from the local, atomic-like features) on an equal footing is necessary to obtain consistent results. The EELS at very low energy are well described by a Drude fit, but features like the damped plasmon peak at $\omega/D \simeq 1.0$ are distinctly non-Drude-like, and can only be reliably accessed by the full analysis, as described above.

Given the above, we expect small coherence-destroying perturbations to tilt the balance in favour of low-energy incoherence. Consideration of doping-induced static disorder has precisely such an effect on the low-energy EELS spectrum. Consistently with the disorder-induced smearing of the Drude part in $\sigma_{xx}(\omega)$, the coherent part in the EELS spectrum is replaced by a broad peak, which still shows remnants of the coherent peak at $v = 0$ ($v = U/4$). However, the low-energy ω^2-dependence in the pure case is replaced by a *linear* ω-dependence in this case. The complete destruction of the quasiparticle behaviour in the DOS and the Drude-like response at $v = U/3$ is consistent with the complete destruction of the 'coherent'

peak in the EELS spectrum; we understand this as overdamping of the collective p–h peak by disorder-induced strong scattering as v is increased. In the strong-disorder regime, the metallic state is incoherent with a pseudogap feature in the DOS [10], and the action of the potential $V_{kk'}$ between the Hubbard band states does not create well-defined elementary excitations, leading to an incoherent response at low energy.

In experiments carried out on the cuprates in their normal state, a very broad plasmon peak is revealed [11], implying poorly defined plasmon excitations in the correlated metallic state. These studies also reveal that the optic 'plasmon' disperses quadratically (in q). Recent studies indicate an acoustic-like heavily damped plasmon mode at small $\boldsymbol{q}$ [12] with a *linear* ω-dependence in $Bi_2Sr_2CaCu_2O_8$, along with a single broad peak. We cannot directly compare our results to those of [12]; the EELS experiment was carried out in the reflection mode, and this measures the quantity $\mathrm{Im}\, g(0, \omega)$, which is not directly related to what we have calculated here. However, looking at the results of [11], we see that the essential features seen there are indeed reproduced by our calculation. To make contact between our calculations and experiments, we shall suppose that the one-band Hubbard model is understood to be the *effective* model describing the coupled-spin-carrier dynamics in the Cu–O planes. We will also assume that band-structure effects are not crucial to the case under study, and that the source of the anomalous behaviours is rooted in the dynamical effects of the strong, local Hubbard interaction, an assumption well supported at doping levels near the optimal one [13]. We stress that the above conditions will be modified in the pseudogap phase, where the precursor effects of d-wave pairing fluctuations—intrinsically non-local—are appreciable [14]. In this doping range, the dynamical effects of non-local correlations will probably lead to even stronger deviations from a FL picture, though a concrete calculation including such effects remains to be developed. With these caveats in mind, we find good qualitative agreement between our results for $v = U/3$ of figure 3 and the experimental EELS lineshapes [11]: the quadratic (in ω) behaviour at low ω, the broad 'plasmon' peak (strongly damped), the asymmetric lineshape, and the continuum response at higher energy are all reproduced in qualitative agreement with experiment. It would be interesting to check whether the plasmon peak shifts to lower energies with hole doping; this would be an interesting check on the validity of the approach presented here. The comparison is quite good up to $\omega/D \simeq 3.0$, beyond which the simple single-band modelling does not apply anyway.

There is extensive experimental work [15] indicating that the metallic phase above T_c near optimal doping in cuprates is not describable in terms of Landau Fermi-liquid ideas. Prelovsek *et al* [16] have recently considered the question of the EELS lineshape in the t–J model, making use of results obtained from finite-temperature Lanczos techniques. Within our approach, it is known that the metallic state away from $n = 1$ above the lattice coherence scale, T_{coh}, is not a Fermi liquid [5]; the calculation carried out above is then consistent with the non-FL charge dynamics if T_{coh} can be driven sufficiently low (below $0.01D$ used here). A very low T_{coh} near $n = 1$ for U/D near the Mott transition is precisely what we expected [5]. Comparing our results with those found in [16], we observe that our results are in nice agreement with those of [17], but the results presented here are more transparent, being based on an analytical scheme. In addition, the results show that the $d = \infty$ approach is capable of producing the low- and high-energy features on the same footing, and, moreover, permits us to include effects of doping-induced static disorder in a consistent way. In view of this, we believe that the approach described here should also be applicable to a wide variety of doped transition metal oxides, where the combined effects of correlations and disorder are especially pronounced [2]. Additionally, effects of orbital degeneracy, etc, in real materials can be treated by a suitable generalization of the above procedure [5]. This is a non-trivial problem, because the solution of the impurity model is harder. We hope to address this issue in future work.

In conclusion, we have considered the energy-loss function of a model for transition metal oxides, and captured the effects of strong, local correlations and static disorder in a consistent way. Comparison of our results with the experimental EELS spectra for cuprates in the 'normal' state above T_c near optimal doping shows that all the main observed features are consistently reproduced by our calculation.

Acknowledgments

LC was supported by the Fundação de Amparo à Pesquisa do Estado de São Paulo (FAPESP). MSL thanks Professor E Müller-Hartmann for encouragement and advice and Professor G Sawatzky for a discussion of the experimental results. MSL was supported by the SfB 341 of the DPG.

References

[1] Tanner D B *et al* 1992 *Physical Properties of High Temperature Superconductors III* ed D M Ginsberg (Singapore: World Scientific) p 363
[2] Imada M *et al* 1999 *Rev. Mod. Phys.* **70** 1039
[3] Pines D and Nozières P 1966 *The Theory of Quantum Liquids* vol 1 (New York: Benjamin)
[4] For a good theoretical review of the Hall effect in strongly correlated systems, see
Shastry B S *et al* 1993 *Phys. Rev. Lett.* **70** 2004
Shastry B S *et al* 1993 *Phys. Rev. Lett.* **71** 2838
[5] Georges A *et al* 1996 *Rev. Mod. Phys.* **68** 13
[6] Dobrosavljevic V *et al* 1992 *Phys. Rev. Lett.* **69** 1113
Miranda E *et al* 1997 *Phys. Rev. Lett.* **78** 290
Laad M S *et al* 2000 *Phys. Rev.* B submitted
(Laad M S *et al* 1999 *Preprint* cond-mat 9911378)
[7] Khurana A 1990 *Phys. Rev. Lett.* **64** 1990
[8] Cox D 1996 *Proc. Workshop on Non-Fermi Liquids; J. Phys.: Condens. Matter* **8**
[9] For a review of the different techniques used to solve the impurity problem in the large-d context, see
Georges A *et al* 1996 *Rev. Mod. Phys.* **68** 13
[10] Laad M S *et al* 1999 *Preprint* cond-mat 9907328
[11] See, for example,
Bozovic I 1990 *Phys. Rev.* B **42** 1969
and see also
Nücker N *et al* 1989 *Phys. Rev.* B **39** 12 379
[12] Schulte K *et al* 1999 unpublished
I thank Professor G Sawatzky for a discussion of the EELS lineshapes for the normal, near-optimally doped $Bi_2Sr_2CaCu_2O_8$ superconductor.
[13] This fact underlies the success of the marginal Fermi-liquid phenomenology in providing an understanding of many aspects of normal-state data for cuprates near optimal doping. The approach is characterized by a predominantly local, anomalous collective susceptibility and self-energy, justifying the use of the $d = \infty$ approximation used here; see, e.g.,
Varma C M *et al* 1989 *Phys. Rev. Lett.* **63** 1996
[14] The dynamical effects of d-wave pair fluctuations, shown to be important in the pseudogap phase in the underdoped region of the phase diagram of cuprates, by Randeria (Varenna Lectures)—see
Randeria M 1997 *Preprint* cond-mat 9711232
are intrinsically non-local, and hence are beyond the scope of the theories based on $d = \infty$.
[15] A vast literature exists, but a complete picture for the breakdown of Fermi-liquid ideas in the normal state of cuprates is given by
Anderson P W 1997 *The Theory of High-T_c Superconductivity in Cuprates* (Princeton, NJ: Princeton University Press)
[16] Prelovsek P *et al* 1999 *Phys. Rev.* B **60** R3735